Detecting Genomic Signatures of Natural Selection with Principal Component Analysis: Application to the 1000 Genomes Data

Nicolas Duforet-Frebourg,[1,2,3] Keurcien Luu,[1,2] Guillaume Laval,[4,5] Eric Bazin,[6] and Michael G.B. Blum*,[1,2]

[1]TIMC-IMAG UMR 5525, Univ. Grenoble Alpes, Grenoble, France

[2]CNRS, TIMC-IMAG, Grenoble, France

[3]Department of Integrative Biology, University of California, Berkeley

[4]Department of Genomes and Genetics, Institut Pasteur, Human Evolutionary Genetics, Paris, France

[5]Centre National De La Recherche Scientifique, URA3012, Paris, France

[6]CNRS, Laboratoire D'ecologie Alpine UMR 5553, Univ. Grenoble Alpes, Grenoble, France

*Corresponding author: E-mail: michael.blum@imag.fr.

Associate editor: John Novembre

Abstract

To characterize natural selection, various analytical methods for detecting candidate genomic regions have been developed. We propose to perform genome-wide scans of natural selection using principal component analysis (PCA). We show that the common F_{ST} index of genetic differentiation between populations can be viewed as the proportion of variance explained by the principal components. Considering the correlations between genetic variants and each principal component provides a conceptual framework to detect genetic variants involved in local adaptation without any prior definition of populations. To validate the PCA-based approach, we consider the 1000 Genomes data (phase 1) considering 850 individuals coming from Africa, Asia, and Europe. The number of genetic variants is of the order of 36 millions obtained with a low-coverage sequencing depth ($3\times$). The correlations between genetic variation and each principal component provide well-known targets for positive selection (EDAR, SLC24A5, SLC45A2, DARC), and also new candidate genes (APPBPP2, TP1A1, RTTN, KCNMA, MYO5C) and noncoding RNAs. In addition to identifying genes involved in biological adaptation, we identify two biological pathways involved in polygenic adaptation that are related to the innate immune system (beta defensins) and to lipid metabolism (fatty acid omega oxidation). An additional analysis of European data shows that a genome scan based on PCA retrieves classical examples of local adaptation even when there are no well-defined populations. PCA-based statistics, implemented in the *PCAdapt* R package and the *PCAdapt fast* open-source software, retrieve well-known signals of human adaptation, which is encouraging for future whole-genome sequencing project, especially when defining populations is difficult.

Key words: FST, principal component analysis, population structure, population genomics, landscape genetics, selection scan, local adaptation, 1000 genomes.

Significance Statement

Positive natural selection or local adaptation is the driving force behind the adaption of individuals to their environment. To identify genomic regions responsible for local adaptation, we propose to consider the genetic markers that are the most related with population structure. To uncover genetic structure, we consider principal component analysis that identifies the primary axes of variation in the data. Our approach generalizes common approaches for genome scan based on measures of population differentiation. To validate our approach, we consider the human 1000 Genomes data and find well-known targets for positive selection as well as new candidate regions. We also find evidence of polygenic adaptation for two biological pathways related to the innate immune system and to lipid metabolism.

Introduction

Because of the flood of genomic data, the ability to understand the genetic architecture of natural selection has dramatically increased. Of particular interest is the study of local positive selection which explains why individuals are adapted to their local environment. In humans, the availability of genomic data fostered the identification of loci involved in positive selection (Sabeti et al. 2007; Barreiro et al. 2008; Pickrell et al. 2009; Grossman et al. 2013). Local positive selection tends to increase genetic differentiation, which can be measured by difference of allele frequencies between populations (Nielsen 2005; Sabeti et al. 2006; Colonna et al. 2014). For instance, a mutation in the DARC gene that confers resistance to malaria is fixed in sub-Saharan African populations whereas it is absent elsewhere (Hamblin et al. 2002). In

Open Access

addition to the variants that confer resistance to pathogens, genome scans also identify other genetic variants, and many of these are involved in human metabolic phenotypes and morphological traits (Barreiro et al. 2008; Hancock et al. 2010).

In order to provide a list of variants potentially involved in natural selection, genome scans compute measures of genetic differentiation between populations and consider that extreme values correspond to candidate regions (Luikart et al. 2003). The most widely used index of genetic differentiation is the F_{ST} index which measures the amount of genetic variation that is explained by variation between populations (Excoffier et al. 1992). However the F_{ST} statistic requires to group individuals into populations which can be problematic when ascertainment of population structure does not show well-separated clusters of individuals (e.g., Novembre et al. 2008). Other statistics related to F_{ST} have been derived to reduce the false discovery rate (FDR) obtained with F_{ST} but they also work at the scale of populations (Bonhomme et al. 2010; Fariello et al. 2013; Günther and Coop 2013). Grouping individuals into populations can be subjective, and important signals of selection may be missed with an inadequate choice of populations (Yang et al. 2012). We have previously developed an individual-based approach for selection scan based on a Bayesian factor model but the Markov chain Monte Carlo (MCMC) algorithm required for model fitting does not scale well to large data sets containing a million of variants or more (Duforet-Frebourg et al. 2014).

We propose to detect candidates for natural selection using principal component analysis (PCA). PCA is a technique of multivariate analysis used to ascertain population structure (Patterson et al. 2006). PCA decomposes the total genetic variation into K axes of genetic variation called principal components. In population genomics, the principal components can correspond to evolutionary processes such as evolutionary divergence between populations (McVean 2009). Using simulations of an island model and of a model of population fission followed by isolation, we show that the common F_{ST} statistic corresponds to the proportion of variation explained by the first K principal components when K has been properly chosen. With this point of view, the F_{ST} of a given variant is obtained by summing the squared correlations of the first K principal components opening the door to new statistics for genome scans. At a genome-wide level, it is known that there is a relationship between F_{ST} and PCA (McVean 2009), and our simulations show that the relationship also applies at the level of a single variant.

The advantages of performing a genome scan based on PCA are multiple: it does not require to group individuals into populations, the computational burden is considerably reduced compared with genome scan approaches based on MCMC algorithms (Foll and Gaggiotti 2008; Riebler et al. 2008; Günther and Coop 2013; Duforet-Frebourg et al. 2014), and candidate single nucleotide polymorphisms (SNPs) can be related to different evolutionary events that correspond to the different principal components. Using simulations and the 1000 Genomes data, we show that PCA can provide useful insights for genome scans. Looking at the correlations between SNPs and principal components provides a novel conceptual framework to detect genomic regions that are candidates for local adaptation.

New Method

New Statistics for Genome Scan

We denote by $\mathbf{Y}$ the $(n \times p)$ centered and scaled genotype matrix where n is the number of individuals and p is the number of loci. The new statistics for genome scan are based on PCA. The objective of PCA is to find a new set of orthogonal variables called the principal components, which are linear combinations of (centered and standardized) allele counts, such that the projections of the data onto these axes lead to an optimal summary of the data. To present the method, we introduce the truncated singular value decomposition (SVD) that approximates the data matrix $\mathbf{Y}$ by a matrix of smaller rank

$$\mathbf{Y} \approx U\Sigma\mathbf{V}^T,$$

where $\mathbf{U}$ is a $(n \times K)$ orthonormal matrix, $\mathbf{V}$ is a $(p \times K)$ orthonormal matrix, Σ is a diagonal $(K \times K)$ matrix and K corresponds to the rank of the approximation. The solution of PCA with K components can be obtained using the truncated SVD: the K columns of $\mathbf{V}$ contain the coefficients of the new orthogonal variables, the K columns of $\mathbf{U}$ contain the projections (called "scores") of the original variables onto the principal components and capture population structure (supplementary fig. S1, Supplementary Material online), and the squares of the elements of Σ are proportional to the proportion of variance explained by each principal component (Jolliffe 2005). We denote the diagonal elements of Σ by $\sqrt{\lambda_k}$, $k = 1, \ldots, K$ where the λ_k's are the ranked eigenvalues of the matrix $\mathbf{YY}^T$. Denoting by $\mathbf{V}_{jk}$, the entry of $\mathbf{V}$ at the jth line and k^{th} column, then the correlation ρ_{jk} between the jth SNP and the kth principal component is given by $\rho_{jk} = \sqrt{\lambda_k}V_{jk}/\sqrt{n-1}$ (Cadima and Jolliffe 1995). In the following, the statistics ρ_{jk} are referred to as "loadings" and will be used for detecting selection.

The second statistic we consider for genome scan corresponds to the proportion of variance of a SNP that is explained by the first K PCs. It is called the communality in exploratory factor analysis because it is the variance of observed variables accounted for by the common factors, which correspond to the first K PCs. Because the principal components are orthogonal to each other, the proportion of variance explained by the first K principal components is equal to the sum of the squared correlations with the first K principal components. Denoting by h_j^2 the communality of the jth SNP, we have

$$h_j^2 = \sum_{k=1}^{K} \rho_{jk}^2.$$

The last statistic we consider for genome scans sums the squared of normalized loadings. It is defined as $h_j'^2 = \sum_{k=1}^{K} V_{jk}^2$. Compared to the communality h^2, the statistic h'^2

should theoretically give the same importance to each PC because the normalized loadings are on the same scale as we have $\sum_{j=1}^{p} V_{jk}^2 = 1$, for $k = 1 \dots K$.

Numerical Computations

The method of selection scan should be able to handle a large number p of genetic variants. In order to compute truncated SVD with large values of p, we compute the $n \times n$ covariance matrix $\Omega = \mathbf{Y}\mathbf{Y}^T/(p-1)$. The covariance matrix Ω is typically of much smaller dimension than the $p \times p$ covariance matrix. Considering the $n \times n$ covariance matrix Ω speeds up matrix operations. Computation of the covariance matrix is the most costly operation and it requires a number of arithmetic operations proportional to pn^2. After computing the covariance matrix Ω, we compute its first K eigenvalues and eigenvectors to find $\Sigma^2/(p-1)$ and $\mathbf{U}$. Eigenanalysis is performed with the *dsyevr* routine of the linear algebra package LAPACK (Anderson et al. 1999). The matrix $\mathbf{V}$, which captures the relationship between each SNPs and population structure, is obtained by the matrix operation $\mathbf{V}^T = \Sigma^{-1}\mathbf{U}^T\mathbf{Y}$. The software *PCAdapt fast*, process data as a stream and never store in order to have a very low memory access whatever the size of the data.

Results

Island Model

To investigate the relationship between communality h^2 and F_{ST}, we consider an island model with three islands. We use $K = 2$ when performing PCA because there are three islands. We choose a value of the migration rate that generates a mean F_{ST} value (across the 1,400 neutral SNPs) of 4%. We consider five different simulations with varying strengths of selection for the 100 adaptive SNPs. In all simulations, the R^2 correlation coefficient between h^2 and F_{ST} is larger than 98%. Considering as candidate SNPs the 1% of the SNPs with largest values of F_{ST} or of h^2, we find that the overlap coefficient between the two sets of SNPs is comprised between 88% and 99%. When varying the strength of selection for adaptive SNPs, we find that the relative difference of FDRs obtained with F_{ST} (top 1%) and with h^2 (top 1%) is smaller than 5%. The similar values of FDR obtained with h^2 and with F_{ST} decrease for increasing strength of selection (supplementary fig. S2, Supplementary Material online).

Divergence Model

To compare the performance of different PCA-based summary statistics, we simulate genetic variation in models of population divergence. The divergence models assume that there are three populations, A, B_1 and B_2 with B_1 and B_2 being the most related populations (figs. 1 and 2). The first simulation scheme assumes that local adaptation took place in the lineages corresponding to the environments of populations A and B_1 (fig. 1). The SNPs, which are assumed to be independent, are divided into three groups: 9,500 SNPs evolve neutrally, 250 SNPs confer a selective advantage in the environment of A, and 250 other SNPs confer a selective

advantage in the environment of B_1. Genetic differentiation, measured by pairwise F_{ST}, is equal to 14% when comparing population A to the other ones and is equal to 5% when comparing populations B_1 and B_2. Performing PCA with $K = 2$ shows that the first component separates population A from B_1 and B_2 whereas the second component separates B_1 from B_2 (supplementary fig. S1, Supplementary Material online). The choice of $K = 2$ is evident when looking at the scree plot because the eigenvalues, which are proportional to the proportion of variance explained by each PC, drop beyond $K = 2$ and stay almost constant as K further increases (supplementary fig. S3, Supplementary Material online).

We investigate the relationship between the communality statistic h^2, which measures the proportion of variance explained by the first two PCs, and the F_{ST} statistic. We find a squared Pearson correlation coefficient between the two statistics larger than 98.8% in the simulations corresponding to figures 1 and 2 (supplementary fig. S4, Supplementary Material online). For these two simulations, we look at the SNPs in the top 1% (respectively, 5%) of the ranked lists based on h^2 and F_{ST}, and we find an overlap coefficient always larger than 93% for the lists provided by the two different statistics (respectively, 95%). Providing a ranking of the SNPs almost similar to the ranking provided by F_{ST} is therefore possible without considering that individuals originate from predefined populations.

We then compare the performance of the different statistics based on PCA by investigating if the top-ranked SNPs (top 1%) manage to pick SNPs involved in local adaptation (fig. 1). The squared loadings ρ_{j1}^2 with the first PC pick SNPs involved in selection in population A (39% of the top 1%), a few SNPs involved in selection in B_1 (9%), and many false positive SNPs (FDR of 53%). The squared loadings with the second PC ρ_{j2}^2 pick less false positives (FDR of 12%) and most SNPs are involved in selection in B_1 (88%) with just a few involved in selection in A (1%). When adaptation took place in two different evolutionary lineages of a divergence tree between populations, a genome scan based on PCA has the nice property that outlier loci correlated with PC1 or with PC2 correspond to adaptive constraints that occurred in different parts of the tree.

Because the communality h^2 gives more importance to the first PC, it picks preferentially the SNPs that are the most correlated with PC1. There is a large overlap of 72% between the 1% top-ranked lists provided by h^2 and ρ_{j1}^2. Therefore, the communality statistic h^2 is more sensitive to ancient adaptation events that occurred in the environment of population A. In contrast, the alternative statistic h'^2 is more sensitive to recent adaptation events that occurred in the environment of population B_1. When considering the top-ranked 1% of the SNPs, h'^2 captures only one SNP involved in selection in A (1% of the top 1%) and 88 SNPs related to adaptation in B_1 (88% of the top 1%). The overlap between the 1% top-ranked lists provided by h'^2 and by ρ_{j2}^2 is of 86%.

The h'^2 statistic is mostly influenced by the second principal component because the distribution of squared loadings corresponding to the second PC has a heavier tail, and this result holds for the two divergence models and for the 1000

Genomes data (supplementary fig. S5, Supplementary Material online). To summarize, the h^2 and h'^2 statistics give too much importance to PC1 and PC2, respectively, and they fail to capture in an equal manner both types of adaptive events occurring in the environment of populations A and B_1.

We also investigate a more complex simulation in which adaptation occurs in the four branches of the divergence tree (fig. 2). Among the 10,000 simulated SNPs, we assume that there are four sets of 125 adaptive SNPs with each set being related to adaptation in one of the four branches of the divergence tree. Compared with the simulation of figure 1, we find the same pattern of population structure (supplementary fig. S1, Supplementary Material online). The squared loadings ρ_{j1}^2 with the first PC mostly pick SNPs involved in selection in the branch that predates the split between B_1 and B_2 (51% of the top 1%), SNPs involved in selection in the environment of population A (9%), and false positive SNPs (FDR of 38%). Except for false positives (FDR of 14%), the squared loadings ρ_{j2}^2 with the second PC rather pick SNPs involved in selection in B_1 and B_2 (42% for B_1 and 44% for B_2). Once again, there is a large overlap between the SNPs picked by the communality h^2 and by ρ_1^2 (92% of overlap) and between the SNPs picked by h'^2 and ρ_2^2 (93% of overlap). Because the first PC discriminates population A from B_1 and B_2 (supplementary fig. S1, Supplementary Material online), the SNPs most correlated with PC1 correspond to SNPs related to adaptation in the (red and green) branches that separate A from populations B_1 and B_2. In contrast, the SNPs that are most correlated to PC2 correspond to SNPs related to adaptation in the two (blue and yellow) branches that separate population B_1 from B_2 (fig. 2).

We additionally evaluate to what extent the results are robust with respect to some parameter settings. When considering the 5% of the SNPs with most extreme values of the statistics instead of the top 1%, we also find that the summary statistics pick SNPs related to different evolutionary events (supplementary fig. S6, Supplementary Material online). The main difference being that the FDR increases considerably when considering the top 5% instead of the top 1% (supplementary fig. S6, Supplementary Material online). We also consider variation of the selection coefficient ranging from $s = 1.01$ to $s = 1.1$ ($s = 1.025$ corresponds to the simulations of figs. 1 and 2). As expected, the FDR of the different statistics based on PCA is considerably reduced when the selection coefficient increases (supplementary fig. S7, Supplementary Material online).

In the divergence model of figure 1, we also compare the FDRs obtained with the statistics h^2, h'^2, and with a Bayesian factor model implemented in the software *PCAdapt* (Duforet-Frebourg et al. 2014). For the optimal choice of $K = 2$, the statistic h'^2 and the Bayesian factor model provide the smallest FDR (supplementary fig. S8, Supplementary Material online). However, when varying the value of K from $K = 1$ to $K = 6$, we find that the communality h^2 and the Bayesian approach are robust to overspecification of K ($K > 3$) whereas the FDR obtained with h'^2 increases importantly as K

increases beyond $K = 2$ (supplementary fig. S8, Supplementary Material online).

We also consider a more general isolation-with-migration model. In the divergence model where adaptation occurs in two different lineages of the population tree (fig. 1), we add constant migration between all pairs of populations. We assume that migration occurred after the split between B_1 and B_2. We consider different values of migration rates generating a mean F_{ST} of 7.5% for the smallest migration rate to a mean F_{ST} of 0% for the largest migration rate. We find that the R^2 correlation between F_{ST} and h^2 decreases as a function of the migration rate (supplementary fig. S9, Supplementary Material online). For F_{ST} values larger than 0.5%, R^2 is larger than 97%. The squared correlation R^2 decreases to 47% for the largest migration rate. Beyond a certain level of migration rate, population structure, as ascertained by principal components, is no more described by well-separated clusters of individuals (supplementary fig. S10, Supplementary Material online) but by a more clinal or continuous pattern (supplementary fig. S10, Supplementary Material online) explaining the difference between F_{ST} and h^2. However, the FDRs obtained with the different statistics based on PCA and with F_{ST} evolve similarly as a function of the migration rate. For both types of approaches, the FDR increases for larger migration with almost no true discovery (only one true discovery in the top 1% lists) when considering the largest migration rate.

The main results obtained under the divergence models can be described as follows. The principal components correspond to different evolutionary lineages of the divergence tree. The communality statistic h^2 provides similar list of candidate SNPs than F_{ST} and it is mostly influenced by the first principal component which can be problematic if other PCs also convey adaptive events. To counteract this limitation, which can potentially lead to the loss of important signals of selection, we show that looking at the squared loadings with each of the principal components provide adaptive SNPs that are related to different evolutionary events. When adding migration rates between lineages, we find that the main results are unchanged up to a certain level of migration rate. Above this level of migration rate, the relationship between F_{ST} and h^2 does not hold anymore and genome scans based on either PCA or F_{ST} produce a majority of false positives.

1000 Genomes Data

Since we are interested in selective pressures that occurred during the human diaspora out of Africa, we decide to exclude individuals whose genetic makeup is the result of recent admixture events (African Americans, Columbians, Puerto Ricans, and Mexicans). The first three principal components capture population structure whereas the following components separate individuals within populations (fig. 3 and supplementary fig. S11, Supplementary Material online). The first and second PCs ascertain population structure between Africa, Asia, and Europe (fig. 3) and the third principal component separates the Yoruba from the Luhya population (supplementary fig. S11, Supplementary Material online). The decay of eigenvalues suggests to use $K = 2$ because the
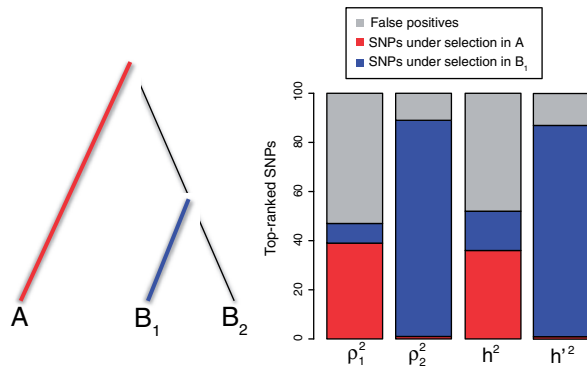
Fig. 1. Repartition of the 1% top-ranked SNPs for each PCA-based statistic under a divergence model with two types of adaptive constraints. Thicker and colored lineages correspond to lineages where adaptation took place. The squared loadings with PC1 ρ_{j1}^2 pick a large proportion of SNPs involved in selection in population A whereas the squared loadings with PC2 ρ_{j2}^2 pick SNPs involved in selection in population B_1. This difference is reflected in the different repartition of the top-ranked SNPs for the communality h^2 and the statistic h'^2.

eigenvalues drop between $K = 2$ and $K = 3$ where a plateau of eigenvalues is reached (supplementary fig. S3, Supplementary Material online).

When performing a genome scan with PCA, there are different choices of statistics. The first choice is the h^2 communality statistic. Using the three continents as labels, there is a squared correlation between h^2 and F_{ST} of $R^2 = 0.989$. To investigate if h^2 is mostly influenced by the first PC, we determine if the outliers for the h^2 statistics are related with PC1 or with PC2. Among the top 0.1% of SNPs with the largest values of h^2, we find that 74% are in the top 0.1% of the squared loadings ρ_{j1}^2 corresponding to PC1 and 20% are in the top 0.1% of the squared loadings ρ_{j2}^2 corresponding to PC2. The second possible choice of summary statistics is the h'^2 statistic. Investigating the repartition of the 0.1% outliers for h', we find that 0.005% are in the top 0.1% of the squared loadings ρ_{j1}^2 corresponding to PC1 and 85% are in the top 0.1% of the squared loadings ρ_{j2}^2 corresponding to PC2. The h'^2 statistic is mostly influenced by the second PC because the distribution of the V_{2j}^2 (normalized squared loadings) has a longer tail than the corresponding distribution for PC1 (supplementary fig. S5, Supplementary Material online). Because the h^2 statistic is mostly influenced by PC1 and h'^2 is mostly influenced by PC2, confirming the results obtained under the divergence models, we rather decide to perform two separate genome scans based on the squared loadings ρ_{j1}^2 and ρ_{j2}^2.

The two Manhattan plots based on the squared loadings for PC1 and PC2 are displayed in figures 4 and 5 (supplementary table S1, Supplementary Material online, contains the loadings for all variants). Because of linkage disequilibrium (LD), Manhattan plots generally produce clustered outliers. To investigate if the top 0.1% outliers are clustered in the genome, we count—for various window sizes—the proportion of contiguous windows containing at least one outlier. We find that outlier SNPs correlated with PC1 or with PC2 are more clustered than expected if they would have been

uniformly distributed among the 36,536,154 variants (supplementary fig. S12, Supplementary Material online). Additionally, the clustering is larger for the outliers related to the second PC as they cluster in fewer windows (supplementary fig. S12, Supplementary Material online). As the genome scan for PC2 captures more recent adaptive events, it reveals larger genomic windows that experienced fewer recombination events.

The 1000 Genome data contain many low-frequency SNPs; 82% of the SNPs have a minor allele frequency smaller than 5%. However, these low-frequency variants are not found among outlier SNPs. There are no SNP with a minor allele frequency smaller than 5% among the 0.1% of the SNPs most correlated with PC1 or with PC2.

The 100 SNPs that are the most correlated with the first PC are located in 24 genomic regions (supplementary table S2, Supplementary Material online). Most of the regions contain just one or a few SNPs except a peak in the gene APPBP2 that contains 33 out of the 100 top SNPs, a peak encompassing the RTTN and CD226 genes containing 17 SNPS and a peak in the ATP1A1 gene containing seven SNPs (fig. 4). Confirming a larger clustering for PC2 outliers, the 100 SNPs that are the most correlated with PC2 cluster in fewer genomic regions (supplementary table S3, Supplementary Material online). They are located in 14 genomic regions including a region overlapping with EDAR contains 44 top hits, two regions containing eight SNPs and located in the pigmentation genes SLC24A5 and SLC45A2, and two regions with seven top hit SNPs, one in the gene KCNMA1 and another one encompassing the RGLA/MYO5C genes (fig. 5).

We perform Gene Ontology (GO) enrichment analyses using *Gowinda* for the SNPs that are the most correlated with PC1 and PC2. For PC1, we find, among others, enrichment (FDR $\leq 5\%$) for ontologies related to the regulation of arterial blood pressure, the endocrine system and the immunity response (interleukin production, response to viruses) (supplementary table S4, Supplementary Material online). For PC2, we find enrichment (FDR $\leq 5\%$) related to olfactory receptors, keratinocyte and epidermal cell differentiation, and ethanol metabolism (supplementary table S5, Supplementary Material online). We also search for polygenic adaptation by looking for biological pathways enriched with outlier genes (Daub et al. 2013). For PC1, we find one enriched (FDR $\leq 5\%$) pathway consisting of the beta defensin pathway (supplementary table S6, Supplementary Material online). The beta defensin pathway contains mainly genes involved in the innate immune system consisting of 36 defensin genes and of two Toll-Like receptors (TLR1 and TLR2). There are additionally two chemokine receptors (CCR2 and CCR6) involved in the beta defensin pathway. For PC2, we also find one enriched pathway consisting of fatty acid omega oxidation (FDR $\leq 5\%$, supplementary table S7, Supplementary Material online). This pathway consists of genes involved in alcohol oxidation (CYP, ALD, and ALDH genes). Performing a less stringent enrichment analysis which can find pathways containing overlapping genes, we find more enriched pathways: the beta defensin and the defensin pathways for PC1 and ethanol oxidation, glycolysis/
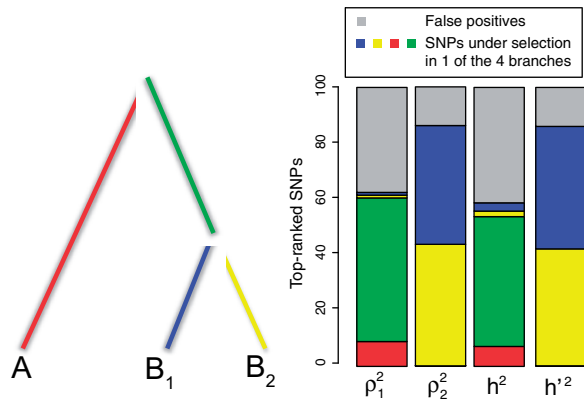
Fig. 2. Repartition of the 1% top-ranked SNPs of each PCA-based statistic under a divergence model with four types of adaptive constraints. Thicker and colored lineages correspond to lineages where adaptation occurred. The different types of SNPs picked by the squared loadings ρ_{j1}^2 and ρ_{j2}^2 is also found when comparing the communality h^2 and the statistic h'^2.

Table 1. Enrichment Measured with Odds Ratio (OR) of the Variants Most Correlated with the Principal Components Obtained from the 1000 Genomes Data.

	Top 0.1%	Top 0.01%	Top 0.005%	Top 100 SNPs
pc1–genic/nogenic	1.60*	1.24	1.09	1.93
pc1–nonsyn/all	1.70	1.18	2.42	10.07*
pc1–UTR/all	1.37	0.80	1.65	3.44
pc2–genic/nogenic	1.51*	2.27	4.73**	4.44*
pc2–nonsyn/all	1.72	4.66*	7.40	12.18*
pc2–UTR/all	1.68	4.01*	3.36	2.73

Note.—Enrichment significant at the 1% (respectively, 5%) level are indicated with ** (resp. *).

gluconeogenesis and fatty acid omega oxidation for PC2 (supplementary table S8, Supplementary Material online).

To further validate the proposed list of candidate SNPs involved in local adaptation, we test for an enrichment of genic or nonsynonymous SNP among the SNPs that are the most correlated with the PC. We measure the enrichment among outliers by computing odds ratio (Kudaravalli et al. 2009; Fagny et al. 2014). For PC1, we do not find significant enrichments (table 1) except when measuring the enrichment of genic regions compared with nongenic regions (OR = 10.18 for the 100 most correlated SNPs, $P < 5\%$ using a permutation procedure). For PC2, we find an enrichment of genic regions among outliers as well as an enrichment of nonsynonymous SNPs (table 1). By contrast with the enrichment of genic regions for SNPs extremely correlated with the first PC, the enrichment for the variants extremely correlated with PC2 outliers is significant when using different thresholds to define outliers (table 1).

Discussion

The promise of a fine characterization of natural selection in humans fostered the development of new analytical methods for detecting candidate genomic regions (Vitti et al. 2013). Population-differentiation based methods such as genome scans based on F_{ST} look for marked differences in allele frequencies between population (Holsinger and Weir 2009). Here, we show that the communality statistic h^2, which measures the proportion of variance of a SNP that is explained by the first K principal components, provides a similar list of outliers than the F_{ST} statistic when there are $K + 1$ populations. In addition, the communality statistic h^2 based on PCA can be viewed as an extension of F_{ST} because it does not require to define populations in advance and can even be applied in the absence of well-defined populations.

To provide an example of genome scans based on PCA when there are no clusters of populations, we additionally consider the POPRES data consisting of 447,245 SNPsyped

for 1,385 European individuals (Nelson et al. 2008). The scree plot indicates that there are $K = 2$ relevant clusters (supplementary fig. S3, Supplementary Material online). The first principal component corresponds to a Southeast–Northwest gradient and the second one discriminates individuals from Southern Europe along a East–West gradient (Novembre et al. 2008; Jay et al. 2013) (fig. 6). Considering the 100 SNPs most correlated with the first PC, we find that 75 SNPs are in the lactase region, 18 SNPs are in the HLA region, 5 SNPs are in the ADH1C gene, 1 SNP is in HERC2, and another is close to the LOC283177 gene (fig. 7). When considering the 100 SNPs most correlated with the second PC, we find less clustering than for PC1 with more peaks (supplementary fig. S13, Supplementary Material online). The regions that contain the largest number of SNPs in the top 100 SNPs are the HLA region (41 SNPs) and a region close to the NEK10 gene (10 SNPs), which is a gene potentially involved in breast cancer (Ahmed et al. 2009). The genome scan retrieves well-known signals of adaption in humans that are related to lactase persistence (LCT) (Bersaglieri et al. 2004), immunity (HLA), alcohol metabolism (ADH1C) (Han et al. 2007), and pigmentation (HERC2) (Wilde et al. 2014). The analysis of the POPRES data shows that genome scan based on PCA can be applied when there is a clinal or continuous pattern of population structure without well-defined clusters of individuals.

When there are clusters of populations, we have shown with simulations that genome scans based on F_{ST} can be reproduced with PCA. Genome scans based on PCA have the additional advantage that a particular axis of genetic variation, which is related to adaptation, can be pinpointed. Bearing some similarities with PCA, performing a spectral decomposition of the kinship matrix has been proposed to pinpoint populations where adaptation took place (Fariello et al. 2013). However, despite of some advantages, the statistical problems related to genome scans with F_{ST} remain. The drawbacks of F_{ST} arise when there is hierarchical population structure or range expansion because F_{ST} does not account for correlations of allele frequencies among subpopulations (Bierne et al. 2013; Lotterhos and Whitlock 2014). An alternative presentation of the issues arising with F_{ST} is that it implicitly assumes either a model of instantaneous divergence between populations or an island-model (Bonhomme et al. 2010). Deviations from these models severely impact FDRs

(Duforet-Frebourg et al. 2014). Viewing F_{ST} from the point of view of PCA provides a new explanation about why F_{ST} does not provide an optimal ranking of SNPs for detecting selection. The statistic F_{ST} or the proposed h^2 communality statistic are mostly influenced by the first principal component and the relative importance of the first PC increases with the difference between the first and second eigenvalues of the covariance matrix of the data. Because the first PC can represent ancient adaptive events, especially under population divergence models (McVean 2009), it explains why F_{ST} and the communality h^2 are biased toward ancient evolutionary events. Following recent developments of F_{ST} -related statistics that account for hierarchical population structure (Bonhomme et al. 2010; Günther and Coop 2013; Foll et al. 2014), we proposed an alternative statistic h'^2, which should give equal weights to the different PCs. However, analyzing simulations and the 1000 Genomes data show that h'^2 do not properly account for hierarchical population structure because outliers identified by h'^2 are almost always related to the last PC kept in the analysis. To avoid to bias data analysis in favor of one principal component, it is possible to perform a genome scan for each principal component.

In addition to ranking the SNPs when performing a genome scan, a threshold should be chosen to extract a list of outlier SNPs. We do not have addressed the question of how to choose the threshold and rather used empirical threshold such as the 99% quantile of the distribution of the test statistic (top 1%). If interested in controlling the FDR, we can assume that the loadings ρ_{kj} are Gaussian with zero mean (Galinsky et al. 2015). Because of the constraints imposed on the loadings when performing PCA, the variance of the ρ_{kj}'s is equal to the proportion of variance explained by the k_{th} PC, which is given by $\lambda_k/(p \times (n-1))$ where λ_k is the k_{th} eigenvalue of the matrix YY^T. Assuming a Gaussian distribution for the loadings, the communality can then be approximated by a weighted sum of chi-square distribution. Approximating a weighted sum of chi-square distribution with a chi-square distribution, we have (Yuan and Bentler 2010)

$$h^2 \times K/c \leadsto \chi_K^2,$$

where $c = \sum_{i=1}^{K} \lambda_K/(p \times (n-1))$ is the proportion of variance explained by the first K PCs. The chi-square approximation of equation (3) bears similarity with the approximation of Lewontin and Krakauer (1973) that states that $F_{ST} \times (n_{pops} - 1)/\bar{F}_{ST}$ follows a chi square approximation with $(n_{pops} - 1)$ degrees of freedom where $\bar{F}_{ST}$ is the mean F_{ST} over loci and n_{pops} is the number of populations. In the simulations of an island model and of a divergence model, quantile-to-quantile plots indicate a good fit to the theoretical chi-square distribution of expression (3) (supplementary fig. S14, Supplementary Material online). When using the chi-square approximation to compute P values, we evaluate if FDR can be controlled using Benjamini–Hochberg correction (Benjamini and Hochberg 1995). We find that the actual proportion of false discoveries corresponds to the target FDR for the island model but the procedure is too conservative for the divergence model (supplementary fig. S15, Supplementary Material online). For

instance, when controlling FDR at a level of 25%, the actual proportion of false discoveries is of 15%. A recent test based on F_{ST} and a chi-square approximation was also found to be conservative (Whitlock and Lotterhos 2015).

Analysing the phase 1 release of the 1000 Genomes data demonstrates the suitability of a genome scan based on PCA to detect signals of positive selection. We search for variants extremely correlated with the first PC, which corresponds to differentiation between Africa and Eurasia and with the second PC, which corresponds to differentiation between Europe and Asia. For variants most correlated with the second PC, there is a significant enrichment of genic and nonsynonymous SNPs whereas the enrichment is less detectable for variants related to the first PC. The enrichment analysis confirms that positive selection may favor local adaptation of human population by increasing differentiation in genic regions especially in nonsynonymous variants (Barreiro et al. 2008). Consistent with LD, we find that candidate variants are clustered along the genome with a larger clustering for variants correlated with the Europe–Asia axis of differentiation (PC2). The difference of clustering illustrates that statistical methods based on LD for detecting selection will perform differently depending on the time frame under which adaptation had the opportunity to occur (Sabeti et al. 2006). The fact that population divergence, and its concomitant adaptive events, between Europe and Asia is more recent that the out-of-Africa event is a putative explanation of the difference of clustering between PC1 and PC2 outliers. Explaining the difference of enrichment between PC1 and PC2 outliers is more difficult. The weaker enrichment for PC1 outliers can be attributed either to a larger number of false discoveries or to a larger importance of other forms of natural selection such as background selection (Hernandez et al. 2011).

When looking at the 100 SNPs most correlated with PC1 or PC2, we find genes for which selection in humans was already documented (9/24 for PC1 and 5/14 for PC2, supplementary table S9, Supplementary Material online). Known targets for selection include genes involved in pigmentation (MATP, OCA2 for PC1 and SLC45A2, SLC24A5, and MYO5C for PC2), in the regulation of sweating (EDAR for PC2), and in adaptation to pathogens (DARC, SLC39A4, and VAV2 for PC1). A 100 kb region in the vicinity of the APPBPP2 gene contains one-third of the 100 SNPs most correlated with PC1. This APPBPP2 region is a known candidate for selection and has been identified by looking for miRNA binding sites with extreme population differentiation (Li et al. 2012). APPBPP2 is a nervous system gene that has been associated with Alzheimer disease, and it may have experienced a selective sweep (Williamson et al. 2007). For some SNPs in APPBPP2, the differences of allele frequencies between Eurasiatic population and sub-Saharan populations from Africa are of the order of 90% (http://popgen.uchicago.edu/ggv/, last accessed December 2015) calling for a further functional analysis. Moreover, looking at the 100 SNPs most correlated with PC1 and PC2 confirms the importance of noncoding RNA (FAM230B, D21S2088E, LOC100133461, LINC00290, LINC01347, LINC00681), such as miRNA (MIR429), as a
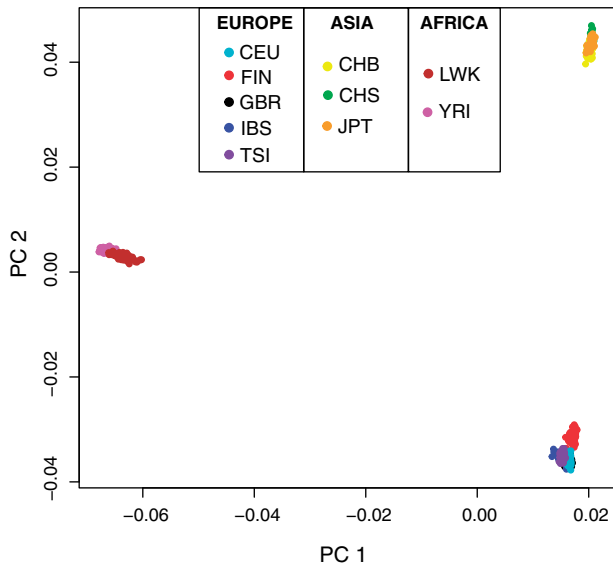
FIG. 3. PCA with $K = 2$ applied to the 1000 Genomes data. The sampled populations are the following: British in England and Scotland (GBR), Utah residents with Northern and Western European ancestry (CEU), Finnish in Finland (FIN), Iberian populations in Spain (IBS), Toscani in Italy (TSI), Han Chinese in Bejing (CHB), Southern Han Chinese (CHS), Japanese in Tokyo (JPT), Luhya in Kenya (LWK), Yoruba in Nigeria (YRI).

substrate for human adaptation (Li et al. 2012; Grossman et al. 2013). Among the other regions with a large number of candidate SNPs, we also found the RTTN/CD226 regions, which contain many SNPs correlated with PC1. In different selection scans, the RTTN genes has been detected (Carlson et al. 2005; Barreiro et al. 2008), and it is involved in the development of the human skeletal system (Wu and Zhang 2010). An other region with many SNPs correlated with PC1 contains the ATP1A1 gene involved in osmoregulation and associated with hypertension (Gurdasani et al. 2015). The regions containing the largest number of SNPs correlated with PC2 are well-documented instances of adaptation in humans and includes the EDAR, SLC24A5, and SLC45A2 genes. The KCNMA1 gene contains seven SNPs correlated with PC2 and is involved in breast cancer and obesity (Jiao et al. 2011; OeggerLi et al. 2012). As for KCNMA1, the MYO5C has already been reported in selection scans although no mechanism of biological adaption has been proposed yet (Chen et al. 2010; Fumagalli et al. 2010). To summarize, the list of most correlated SNPs with the PCs identifies well-known genes related to biological adaptation in humans (EDAR, SLC24A5, SLC45A2, DARC), but also provides candidate genes that deserve further studies such as the APPBPP2, TP1A1, RTTN, KCNMA1, and MYO5C genes, as well as the ncRNAs listed above.

We also show that a scan based on PCA can also be used to detect more subtle footprints of positive selection. We conduct an enrichment analysis that detects polygenic adaptation at the level of biological pathways (Daub et al. 2013). We find that genes in the beta-defensin pathway are enriched in SNPs correlated with PC1. The beta-defensin genes are key components of the innate immune system and have evolved

through positive selection in the catarrhine primate lineages (Hollox and Armour 2008). As for the HLA complex, some beta-defensin genes (DEFB1, DEFB127) show evidence of long-term balancing selection with major haplotypic clades coexisting since millions of years (Cagliani et al. 2008; Hollox and Armour 2008). We also find that genes in the omega fatty acid oxidation pathways are enriched in SNPs correlated with PC2. This pathway was also found when investigating polygenic adaptation to altitude in humans (Foll et al. 2014). The proposed explanation was that omega oxidation becomes a more important metabolic pathway when beta oxidation is defective, which can occur in case of hypoxia (Foll et al. 2014). However, this explanation is not valid in the context of the 1000 Genomes data when there are no populations living in hypoxic environments. Proposing phenotypes on which selection operates is complicated by the fact that the omega fatty acid oxidation pathway strongly overlaps with two other pathways: ethanol oxidation and glycolysis. Evidence of selection on the alcohol dehydrogenase locus have already been provided (Han et al. 2007) with some authors proposing that a lower risk for alcoholism might have been beneficial after rice domestication in Asia (Peng et al. 2010). This hypothesis is speculative and we lack a confirmed biological mechanism explaining the enrichment of the fatty acid oxidation pathway. More generally, the enrichment of the beta-defensin and of the omega fatty acid oxidation pathways confirms the importance of pathogenic pressure and of metabolism in human adaptation to different environments (Hancock et al. 2008; Barreiro and Quintana-Murci 2009; Fumagalli et al. 2011; Daub et al. 2013).

In conclusion, we propose a new approach to scan genomes for local adaptation that works with individual genotype data. Because the method is efficiently implemented in the software *PCAdapt fast*, analyzing 36,536,154 SNPs took only 502 min using a single core of an Intel(R) Xeon(R) (E5-2650, 2.00GHz, 64 bits). Even with low-coverage sequence data ($3\times$), PCA-based statistics retrieve well-known examples of biological adaptation which is encouraging for future whole-genome sequencing project, especially for nonmodel species, aiming at sampling many individuals with limited cost.

Materials and Methods

Simulations of an Island Model

Simulations were performed with *ms* (Hudson 2002). We assume that there are three islands with 100 sampled individuals in each of them. There is a total of 1,400 neutral SNPs, and 100 adaptive SNPs. SNPs are assumed to be unlinked. To mimic adaptation, we consider that adaptive SNP have a migration rate smaller than the migration rate of neutral SNPs ($4N_0m = 4$ for neutral SNPs) (Bazin et al. 2010). The strength of selection is equal to the ratio of the migration rates of neutral and adaptive SNPs. Adaptation is assumed to occur in one population only. The *ms* command lines for neutral and adaptive SNPs are given below (assuming an effective migration rate of $4N_0m = 0.1$ for adaptive SNPs).

```
./ms 300 1400 -s 1 -I 3 100 100 100 -ma x 4 4 4 x
4 4 4 x #neutral.
```
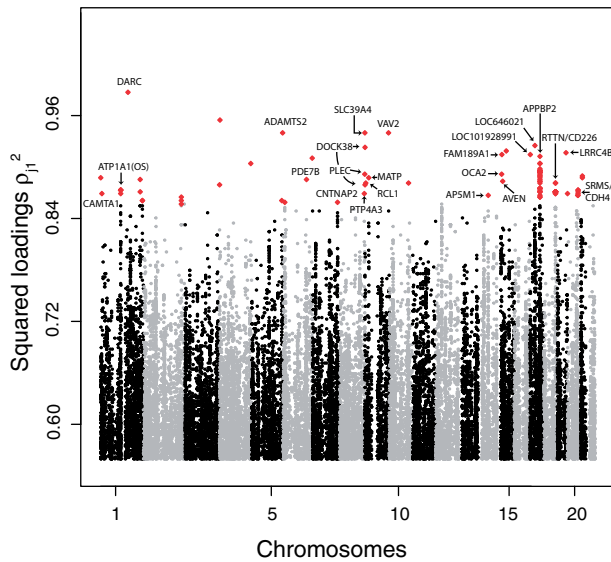
FIG. 4. Manhattan plot for the 1000 Genomes data of the squared loadings ρ^2_{j1} with the first principal component. For sake of presentation, only the top-ranked SNPs (top 0.1%) are displayed and the 100 top-ranked SNPs are colored in red.

FIG. 5. Manhattan plot for the 1000 Genomes data of the squared loadings ρ^2_{j2} with the second principal component. For sake of presentation, only the top-ranked SNPs (top 0.1%) are displayed and the 100 top-ranked SNPs are colored in red.

```
/ms 300 100 -s 1 -I 3 100 100 100 -ma x 0.1 0.1
0.1 x 4 0.1 4 x #outlier
```

The values of migrations rates we consider for adaptive SNPs are $4N_0m = 0.04, 0.1, 0.4, 1, 2$.

Simulations of Divergence Models

We assume that each population has a constant effective population size of $N_0 = 1,000$ diploid individuals, with 50 individuals sampled in each population. The genotypes consist of 10,000 independent SNPs. The simulations were performed in two steps. In the first step, we used the software *ms* to simulate genetic diversity (Hudson 2002) in the ancestral population. We kept only variants with a minor allele frequency larger than 5% at the end of the first step. The second step was performed with *SimuPOP* (Peng and Kimmel 2005) and simulations were started using the allele frequencies generated with *ms* in the ancestral population. Looking forward in time, we consider that there are 100 generations between the initial split and the following split between the two *B* subpopulations, and 200 generations following the split between the two *B* subpopulations. We assume no migration between populations. In the simulation of figure 1, we assume that 250 SNPs confer a selective advantage in the branch leading to population *A* and 250 other SNPs confer a selective advantage in the branch leading to population B_1. We consider an additive model for selection with a selection coefficient of $s = 1.025$ for heterozygotes. For the simulation of figure 2, we assume that there are four nonoverlapping sets of 125 adaptive SNPs with each set being related to adaptation in one of the four branches of the divergence tree. A SNP can confer a selective advantage in a single branch only.

When including migration, we consider that there are 200 generations between the initial split and the following split
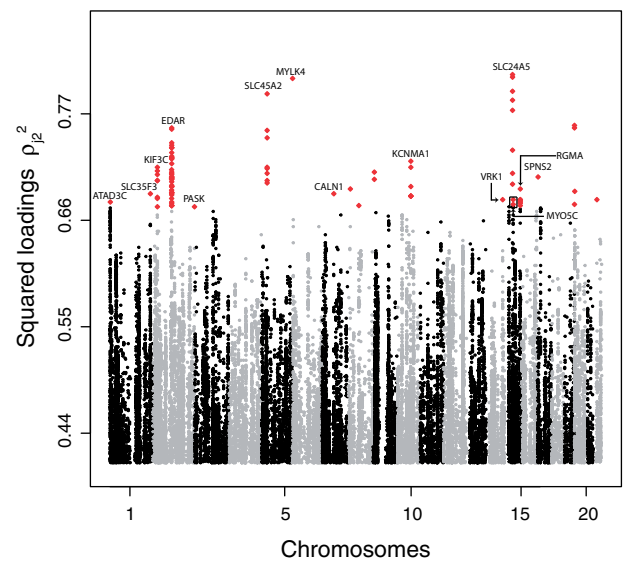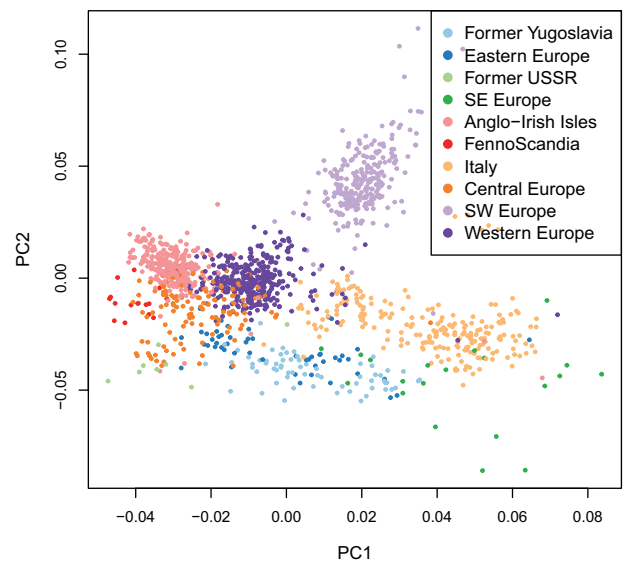

FIG. 6. PCA with $K = 2$ applied to the POPRES data.

between the two *B* subpopulations, and 100 generations following the split between the two *B* subpopulations. We consider migration rates ranging from 0.2% to 5% per generation. Migration is assumed to occur only after the split between B_1 and B_2. The migration rate is the same for the three pairs of populations. To estimate the F_{ST} statistic, we consider the estimator of Weir and Cockerham (1984).

1000 Genomes Data

We downloaded the 1000 Genomes data (phase 1 v3) (The 1000 Genomes Project Consortium 2012). We kept low-coverage genome data and excluded exomes and triome data to minimize variation in read depth. Filtering the data resulted in

Fig. 7. Manhattan plot for the POPRES data of the squared loadings ρ_{j1}^2 with the first principal component. For sake of presentation, only the top-ranked SNPs (top 5%) are displayed and the 100 top-ranked SNPs are colored in red.
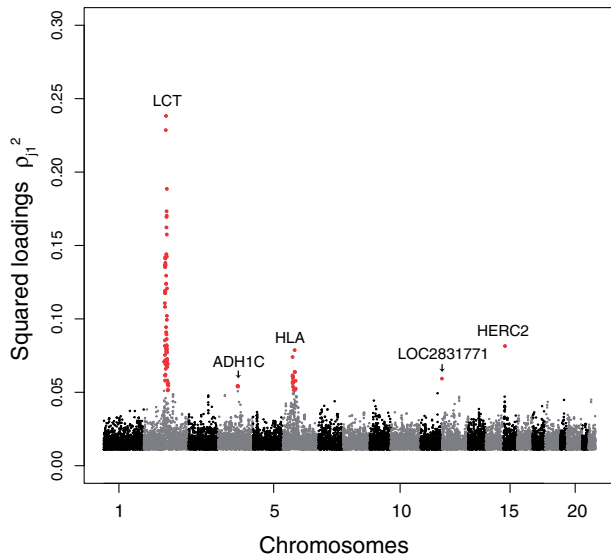
a total of 36,536,154 SNPs that have been typed on 1,092 individuals. Because the analysis focuses on biological adaptation that took place during the human diaspora out of Africa, we removed recently admixed populations (Mexican, Columbian, PortoRican, and AfroAmerican individuals from the Southwest of the United States). The resulting data set contains 850 individuals coming from Asia (two Han Chinese and one Japanese populations), Africa (Yoruba and Luhya), and Europe (Finish, British in England and Scotland, Iberian, Toscan, and Utah residents with Northern and Western European ancestry).

Enrichment Analyses

We used *Gowinda* (Kofler and Schlötterer 2012) to test for enrichment of GO. A gene is considered as a candidate if there is at least one of the most correlated SNPs (top 1%) that is mapped to the gene (within an interval of 50 kb upstream and downstream of the gene). Enrichment was computed as the proportion of genes containing at least one outlier SNPs among the genes of the given GO category that are present in the data set. In order to sample a null distribution for enrichment, *Gowinda* performs resampling without replacement of the SNPs. We used the –*gene* option of *Gowinda* that assumes complete linkage within genes.

We performed a second enrichment analysis to determine if outlier SNPs are enriched for genic regions. We computed odds ratio (Kudaravalli et al. 2009)

$$OR = \frac{Pr(genic \mid outlier)}{Pr(not\ genic \mid outlier)} \frac{Pr(not\ genic \mid not\ outlier)}{Pr(genic \mid not\ outlier)}.$$

We implemented a permutation procedure to test if an odds ratio is significantly larger than 1 (Fagny et al. 2014). The same procedure was applied when testing for enrichment of

UTR regions (untranslated regions) and of nonsynonymous SNPs.

Polygenic Adaptation

To test for polygenic adaptation, we determined whether genes in a given biological pathway show a shift in the distribution of the loadings (Daub et al. 2013). We computed the SUMSTAT statistic for testing if there is an excess of selection signal in each pathway (Daub et al. 2013). We applied the same pruning method to take into account redundancy of genes within pathways. The test statistic is the squared loading standardized into a z-score (Daub et al. 2013). SUMSTAT is computed for each gene as the sum of test statistic of each SNP belonging to the gene. Intergenic SNPs are assigned to a gene provided they are situated 50 kb up- or downstream. We downloaded 63,693 known genes from the UCSC website and we mapped SNPs to a gene if a SNP is located within a gene transcript or within 50 kb of a gene. A total of 18,267 genes were mapped with this approach. We downloaded 2,681 gene sets from the NCBI Biosystems database. After discarding genes that were not part of the aforementioned gene list, removing gene sets with less than 10 genes and pooling nearly identical gene sets, we kept 1,532 sets for which we test if there was a shift of the distribution of loadings.

Supplementary Material

Supplementary figures S1–S15 and tables S1–S9 *Molecular Biology and Evolution* online (http://www.mbe.oxfordjournals.org/).

Acknowledgments

References

Ahmed S, Thomas G, Ghoussaini M, Healey CS, Humphreys MK, Platte R, Morrison J, Maranian M, Pooley KA, Luben R, et al. 2009. Newly discovered breast cancer susceptibility loci on 3p24 and 17q23.2. *Nat Genet.* 41:585–590.

The 1000 Genomes Project Consortium. 2012. An integrated map of genetic variation from 1,092 human genomes. Nature 491:56–65.

Anderson E, Bai Z, Bischof C, Blackford S, Demmel J, Dongarra J, Du Croz J, Greenbaum A, Hammarling S, McKenney A, Sorensen D. 1999. LAPACK users' guide. 3rd edn. Philadelphia (PA): Society for Industrial and Applied Mathematics.

Barreiro LB, Laval G, Quach H, Patin E, Quintana-Murci L. 2008. Natural selection has driven population differentiation in modern humans. *Nat Genet.* 40:340–345.

Barreiro LB, Quintana-Murci L. 2009. From evolutionary genetics to human immunology: how selection shapes host defence genes. *Nat Rev Genet.* 11:17–30.

Bazin E, Dawson KJ, Beaumont MA. 2010. Likelihood-free inference of population structure and local adaptation in a Bayesian hierarchical model. *Genetics* 185:587–602.

Benjamini Y, Hochberg Y. 1995. Controlling the false discovery rate: a practical and powerful approach to multiple testing. *J R Stat Soc Series B Stat Methodol.* 57:289–300.

Bersaglieri T, Sabeti PC, Patterson N, Vanderploeg T, Schaffner SF, Drake JA, Rhodes M, Reich DE, Hirschhorn JN. 2004. Genetic signatures of

strong recent positive selection at the lactase gene. *Am J Hum Genet.* 74:1111–1120.

Bierne N, Roze D, Welch JJ. 2013. Pervasive selection or is it . . . ? why are F_{ST} outliers sometimes so frequent? *Mol Ecol* 22:2061–2064.

Bonhomme M, Chevalet C, Servin B, Boitard S, Abdallah J, Blott S, SanCristobal M. 2010. Detecting selection in population trees: the Lewontin and Krakauer test extended. *Genetics* 186:241–262.

Cadima J, Jolliffe IT. 1995. Loading and correlations in the interpretation of principal components. *J Appl Stat.* 22:203–214.

Cagliani R, Fumagalli M, Riva S, Pozzoli U, Comi GP, Menozzi G, Bresolin N, Sironi M. 2008. The signature of long-standing balancing selection at the human defensin beta-1 promoter. *Genome Biol.* 9:R143.

Carlson CS, Thomas DJ, Eberle MA, Swanson JE, Livingston RJ, Rieder MJ, Nickerson DA. 2005. Genomic regions exhibiting positive selection identified from dense genotype data. *Genome Res.* 15:1553–1565.

Chen H, Patterson N, Reich D. 2010. Population differentiation as a test for selective sweeps. *Genome Res.* 20:393–402.

Colonna V, Ayub Q, Chen Y, Pagani L, Luisi P, Pybus M, Garrison E, Xue Y, Tyler-Smith C, the 1000 Genomes Project Consortium. 2014. Human genomic regions with exceptionally high levels of population differentiation identified from 911 whole-genome sequences. *Genome Biol.* 15:R88.

Daub JT, Hofer T, Cutivet E, Dupanloup I, Quintana-Murci L, Robinson-Rechavi M, Excoffier L. 2013. Evidence for polygenic adaptation to pathogens in the human genome. *Mol Biol Evol.* 30:1544–1558.

Duforet-Frebourg N, Bazin E, Blum MGB. 2014. Genome scans for detecting footprints of local adaptation using a Bayesian factor model. *Mol Biol Evol.* 31:2483–2495.

Excoffier L, Smouse PE, Quattro JM. 1992. Analysis of molecular variance inferred from metric distances among DNA haplotypes: application to human mitochondrial DNA restriction data. *Genetics* 131:479–491.

Fagny M, Patin E, Enard D, Barreiro LB, Quintana-Murci L, Laval G. 2014. Exploring the occurrence of classic selective sweeps in humans using whole-genome sequencing data sets. *Mol Biol Evol.* 31:1850–1868.

Fariello MI, Boitard S, Naya H, SanCristobal M, Servin B. 2013. Detecting signatures of selection through haplotype differentiation among hierarchically structured populations. *Genetics* 193:929–941.

Foll M, Gaggiotti O. 2008. A genome-scan method to identify selected loci appropriate for both dominant and codominant markers: a Bayesian perspective. *Genetics* 180:977–993.

Foll M, Gaggiotti OE, Daub JT, Vatsiou A, Excoffier L. 2014. Widespread signals of convergent adaptation to high altitude in Asia and America. *Am J Hum Genet.* 95:394–407.

Fumagalli M, Pozzoli U, Cagliani R, Comi GP, Bresolin N, Clerici M, Sironi M. 2010. Genome-wide identification of susceptibility alleles for viral infections through a population genetics approach. *PLoS Genet.* 6:e1000849.

Fumagalli M, Sironi M, Pozzoli U, Ferrer-Admettla A, Pattini L, Nielsen R. 2011. Signatures of environmental genetic adaptation pinpoint pathogens as the main selective pressure through human evolution. *PLoS Genet.* 7:e1002355.

Galinsky KJ, Bhatia G, Loh P, Georgiev R, Mukherjee SS, Patterson NJ, Price AL. 2015. Fast principal components analysis reveals convergent evolution of ADH1B gene in Europe and East Asia. *bioRxiv* 018143.

Grossman SR, Andersen KG, Shlyakhter I, Tabrizi S, Winnicki S, Yen A, Park DJ, Griesemer D, Karlsson EK, Wong SH, et al. 2013. Identifying recent adaptations in large-scale genomic data. *Cell* 152:703–713.

Günther T, Coop G. 2013. Robust identification of local adaptation from allele frequencies. *Genetics* 195:205–220.

Gurdasani D, Carstensen T, Tekola-Ayele F, Pagani L, Tachmazidou I, Hatzikotoulas K, Karthikeyan S, Iles L, Pollard MO, Choudhury A, et al. 2015. The African genome variation project shapes medical genetics in Africa. *Nature* 517:327–332.

Hamblin MT, Thompson EE, Di Rienzo A. 2002. Complex signatures of natural selection at the Duffy blood group locus. *Am J Hum Genet.* 70:369–383.

Han Y, Gu S, Oota H, Osier MV, Pakstis AJ, Speed WC, Kidd JR, Kidd KK. 2007. Evidence of positive selection on a class I ADH locus. *Am J Hum Genet.* 80:441–456.

Hancock AM, Witonsky DB, Ehler E, Alkorta-Aranburu G, Beall C, Gebremedhin A, Sukernik R, Utermann G, Pritchard J, Coop G, et al. 2010. Human adaptations to diet, subsistence, and ecoregion are due to subtle shifts in allele frequency. *Proc Natl Acad Sci U S A.* 107:8924–8930.

Hancock AM, Witonsky DB, Gordon AS, Eshel G, Pritchard JK, Coop G, Di Rienzo A. 2008. Adaptations to climate in candidate genes for common metabolic disorders. *PLoS Genet.* 4:e32.

Hernandez RD, Kelley JL, Elyashiv E, Melton SC, Auton A, McVean G, 1000 Genomes Project, Sella G, Przeworski M. 2011. Classic selective sweeps were rare in recent human evolution. *Science* 331:920–924.

Hollox EJ, Armour JA. 2008. Directional and balancing selection in human beta-defensins. *BMC Evol Biol.* 8:113.

Holsinger KE, Weir BS. 2009. Genetics in geographically structured populations: defining, estimating and interpreting FST. *Nat Rev Genet.* 10:639–650.

Hudson RR. 2002. Generating samples under a Wright-Fisher neutral model of genetic variation. *Bioinformatics* 18:337–338.

Jay F, Sjödin P, Jakobsson M, Blum MGB. 2013. Anisotropic isolation by distance: the main orientations of human genetic differentiation. *Mol Biol Evol.* 30:513–525.

Jiao H, Arner P, Hoffstedt J, Brodin D, Dubern B, Czernichow S, van't Hooft F, Axelsson T, Pedersen O, Hansen T, et al. 2011. Genome wide association study identifies KCNMA1 contributing to human obesity. *BMC Med Genomics.* 4:51.

Jolliffe I. 2005. Principal component analysis. Springer: New-York.

Kofler R, Schlötterer C. 2012. Gowinda: unbiased analysis of gene set enrichment for genome-wide association studies. *Bioinformatics* 28:2084–2085.

Kudaravalli S, Veyrieras JB, Stranger BE, Dermitzakis ET, Pritchard JK. 2009. Gene expression levels are a target of recent natural selection in the human genome. *Mol Biol Evol.* 26:649–658.

Lewontin R, Krakauer J. 1973. Distribution of gene frequency as a test of the theory of the selective neutrality of polymorphisms. *Genetics* 74:175–195.

Li J, Liu Y, Xin X, Kim TS, Cabeza EA, Ren J, Nielsen R, Wrana JL, Zhang Z. 2012. Evidence for positive selection on a number of MicroRNA regulatory interactions during recent human evolution. *PLoS Genet.* 8:e1002578.

Lotterhos KE, Whitlock MC. 2014. Evaluation of demographic history and neutral parameterization on the performance of F_{ST} outlier tests. *Mol Ecol.* 23:2178–2192.

Luikart G, England PR, Tallmon D, Jordan S, Taberlet P. 2003. The power and promise of population genomics: from genotyping to genome typing. *Nat Rev Genet.* 4:981–994.

McVean G. 2009. A genealogical interpretation of principal components analysis. *PLoS Genet.* 5:e1000686.

Nelson MR, Bryc K, King KS, Indap A, Boyko AR, Novembre J, Briley LP, Maruyama Y, Waterworth DM, Waeber G, et al. 2008. The population reference sample, POPRES: a resource for population, disease, and pharmacological genetics research. *Am J Hum Genet.* 83:347–358.

Nielsen R. 2005. Molecular signatures of natural selection. *Annu Rev Genet.* 39:197–218.

Novembre J, Johnson T, Bryc K, Kutalik Z, Boyko AR, Auton A, Indap A, King KS, Bergmann S, Nelson MR, et al. 2008. Genes mirror geography within Europe. *Nature* 456:98–101.

Oeggerli M, Tian Y, Ruiz C, Wijker B, Sauter G, Obermann E, Güth U, Zlobec I, Sausbier M, Kunzelmann K, et al. 2012. Role of KCNMA1 in breast cancer. *PLoS One* 7:e41664.

Patterson N, Price AL, Reich D. 2006. Population structure and eigenanalysis. *PLoS Genet.* 2:e190.

Peng B, Kimmel M. 2005. simuPOP: a forward-time population genetics simulation environment. *Bioinformatics* 21:3686–3687.

Peng Y, Shi H, Qi Xb, Xiao Cj, Zhong H, Run-lin ZM, Su B. 2010. The ADH1B Arg47His polymorphism in East Asian populations and expansion of rice domestication in history. *BMC Evol Biol.* 10:15.

Pickrell JK, Coop G, Novembre J, Kudaravalli S, Li JZ, Absher D, Srinivasan BS, Barsh GS, Myers RM, Feldman MW, et al. 2009. Signals of recent positive selection in a worldwide sample of human populations. *Genome Res.* 19:826–837.

Riebler A, Held L, Stephan W. 2008. Bayesian variable selection for detecting adaptive genomic differences among populations. *Genetics* 178:1817–1829.

Sabeti P, Schaffner S, Fry B, Lohmueller J, Varilly P, Shamovsky O, Palma A, Mikkelsen T, Altshuler D, Lander E. 2006. Positive natural selection in the human lineage. *Science* 312:1614–1620.

Sabeti PC, Varilly P, Fry B, Lohmueller J, Hostetter E, Cotsapas C, Xie X, Byrne EH, McCarroll SA, Gaudet R, et al. 2007. Genome-wide detection and characterization of positive selection in human populations. *Nature* 449:913–918.

Vitti JJ, Grossman SR, Sabeti PC. 2013. Detecting natural selection in genomic data. *Annu Rev Genet.* 47:97–120.

Weir BS, Cockerham CC. 1984. Estimating F-statistics for the analysis of population structure. *Evolution* 1358–1370.

Whitlock MC, Lotterhos KE. 2015. Reliable detection of loci responsible for local adaptation: inference of a null model through trimming the distribution of F_{ST}. *Am Nat.* 186:S24–S36.

Wilde S, Timpson A, Kirsanow K, Kaiser E, Kayser M, Unterländer M, Hollfelder N, Potekhina ID, Schier W, Thomas MG, et al. 2014. Direct evidence for positive selection of skin, hair, and eye pigmentation in Europeans during the last 5,000 y. *Proc Natl Acad Sci U S A.* 111:4832–4837.

Williamson SH, Hubisz MJ, Clark AG, Payseur BA, Bustamante CD, Nielsen R. 2007. Localizing recent adaptive evolution in the human genome. *PLoS Genet.* 3:e90.

Wu DD, Zhang YP. 2010. Positive selection drives population differentiation in the skeletal genes in modern humans. *Hum Mol Genet.* 19:2341–2346.

Yang WY, Novembre J, Eskin E, Halperin E. 2012. A model-based approach for analysis of spatial structure in genetic data. *Nat Genet.* 44:725–731.

Yuan KH, Bentler PM. 2010. Two simple approximations to the distributions of quadratic forms. *Br J Math Stat Psychol.* 63:273–291.